1999-03

Interaction of plasmas with intense lasers

Kruer, W.L.

Livermore,California. Lawrence Livermore National Laboratory

W.L. Kruer, "Interaction plasmas with intense lasers," 1999 Centennial Meeting, Atlanta, GA March 20-26, 1999, 35 p. (Preprint)
http://hdl.handle.net/10945/52665

UCRL-JC-132222
PREPRINT

Interaction of Plasmas with Intense Lasers

W. L. Kruer

This paper was prepared for submittal to the
1999 Centennial Meeting
Atlanta, GA
March 20-26, 1999

April 30, 1999

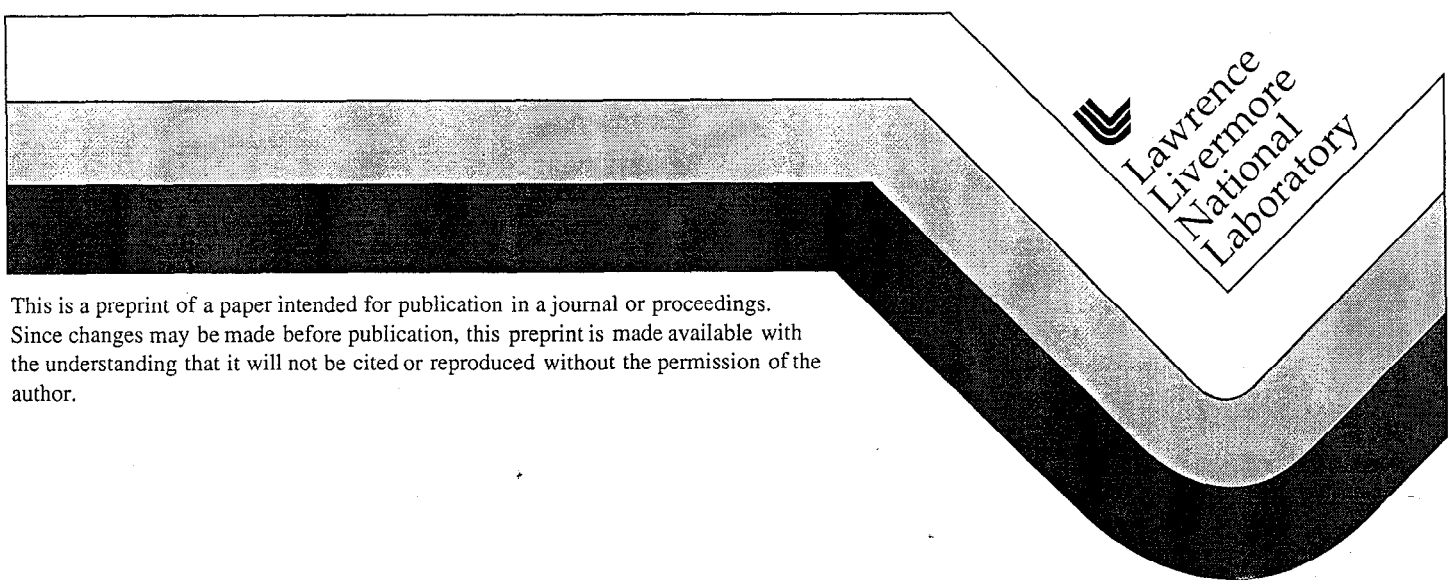

Interaction of plasmas with intense lasers

William L. Kruer
Naval Postgraduate School, Monterey, CA 93943 and
Lawrence Livermore National Laboratory, Livermore, CA 94550

The interaction of plasmas with intense lasers is an excellent example of how different fields of physics are inter-connected. Invention of the laser and its ongoing development has allowed the creation and study of high temperature, dense matter in the laboratory. The results both advance the underlying plasma science and are relevant to many fields ranging from astrophysics to fusion and nonlinear physics. A brief overview of the interaction physics is given. Selected topics are discussed to illustrate the exciting progress in experimental, theoretical and computational investigations with focussed laser intensities up to 10^{21} W/cm^2.

I. INTRODUCTION

Invention of the laser is an excellent example of how the different subfields of physics are inter-connected. High power lasers have become a powerful tool for the creation and study of high temperature matter in the laboratory. These studies have both increased our understanding of the physics of ionized media and have numerous applications ranging from astrophysics to fusion science.

Over the last 25 years, there has been a very impressive development[1] of high power glass lasers in the inertial fusion program. The laser power has increased from a fraction of a terrawatt to a petawatt, the energy from a few joules to soon about two megajoules. This progress is illustrated in Fig. 1, which shows glass lasers developed at the Lawrence Livermore National Laboratory. In 1974, the Janus laser delivered about 10 joules of 1.06μm light in a pulse of about 100 ps. The technology rapidly advanced over the years to the Nova laser which provides about 30 kJ of 0.35 μm light in nanosecond pulses. Using chirped pulse amplification, one beamline of Nova has been used to produce a petawatt short pulse (<1 ps) of 1.06 μm light. Nova will soon be decommissioned as construction of the National Ignition Facility (NIF) proceeds. NIF will provide nearly 2 MJ of 0.35 μm light in pulse lengths of order 10 ns. Other high power glass lasers exist at the University of Rochester, Los Alamos National Laboratory, and throughout the world. A KrF gas laser delivering 0.26 μm light is now operative at the Naval Research Laboratory.

The focus here will be on the interaction of intense lasers with ionized matter, which is a fundamental topic of interest to many areas of science ranging from astrophysics to fusion. The interaction physics is a rich test bed for many

basic processes in plasmas. A brief discussion will be given of important linear and nonlinear optical processes, some of which involve plasma waves and instabilities. Progress will be illustrated by a consideration of three recent examples of the nonlinear interaction physics. These examples are chosen to represent science with small lasers, with large lasers, and with ultra-intense lasers. The irradiation of matter with intense laser light also provides a laboratory for the study of many applications, including inertial fusion, astrophysical phenomena , and many topics in high energy density physics. A very short discussion of some applications will be given. Fortunately, these and other applications such as laser plasma accelerators will be discussed in depth in other papers in this Centennial issue.

II. INTERACTION PHYSICS

Laser plasma interactions are extremely rich and challenging. The coupling processes[2] span the gamut from classical inverse bremssthralung to many nonlinear optical processes, such as stimulated Raman and Brillouin scattering and filamentation. Inverse bremssthralung simply represents collisional absorption as the coherent motion of the electrons in the laser electric field is converted to random thermal motion when the electrons are scattered by the ions. In other words,

$$\nu_{ei}\frac{mv_{os}^2}{2} = \nu\frac{E_L^2}{8\pi}, \qquad (1)$$

where ν is the damping rate, E_L the electric field of the light wave, v_{os} the oscillation velocity of electrons in this field, and ν_{ei} is an electron-ion collision frequency. Stimulated Raman and Brillouin scattering (SRS and SBS) can be most

simply described as the resonant decay of the incident laser light into a scattered light wave plus either a high frequency electron plasma wave or a low frequency sound wave; i.e.,

$$\begin{aligned} \omega_L &\rightarrow \omega_{sc} + \omega_{pe} \quad SRS \\ \omega_L &\rightarrow \omega_{sc} + \omega_{ia} \quad SBS \end{aligned} \tag{2}$$

where ω_L (ω_{sc}) is the frequency of the laser (scattered)light, ω_{pe} is the electron plasma frequency, and ω_i the ion sound frequency. Note that we are considering the simplest case of a plasma with no imposed or self-generated magnetic fields.

Filamentation represents a nonresonant process in which a region of enhanced laser intensity pushes plasma aside, creating a density depression. Light is refracted into the depression, further enhancing the intensity. The resulting instability can lead to break-up of the incident beam into intense filaments. Note that the density depression can be created either directly by the light pressure or indirectly by the plasma pressure due to enhanced heating. For ultra-intense light, the momentum of electrons oscillating in the laser field (p_{os}) can greatly exceed mc, which is the rest mass times the velocity of light. Many relativistic phenomena are then accessed, such as electron heating via the oscillating component of the ponderomotive force and filamentation via relativistic effects.

Virtually all these processes have now been identified and studied in experiments.[3] Many important trends and nonlinear consequences predicted by theory and computer simulation have been confirmed in experiments. One very important nonlinear consequence is the generation of suprathermal electrons via nonlinear optical processes involving electron plasma waves. Important scalings of the nonlinear optical processes have also been established. As predicted, these

processes are more potent in longer scale length plasmas but can be reduced with the use of shorter wavelength light and with the addition of laser beam incoherence. The nonlinear consequences and trends play a vital role in applications. For example, in inertial fusion one needs to minimize the nonlinear optical processes which can lead to capsule preheat, reduced absorption, or inadequate implosion symmetry. The interaction physics then determines the acceptable laser wavelength (≤ 0.35 μm), the beam smoothing characteristics, and various constraints on the acceptable intensity and plasma conditions in the target designs. Of course, in other applications, one may aim to exploit nonlinear processes, such as in laser plasma accelerators.

III. STIMULATED RAMAN SCATTERING

Stimulated Raman Scattering is an excellent example of an important nonlinear optical process. Since the scattered light is downshifted by the electron plasma frequency, this process is easily identified via the spectrum of the scattered light. A representative scattered intensity versus wavelength measured in experiments with 0.35 μm laser light[4] is shown in Fig. 2. Since the electron plasma frequency is a function of plasma density, the spectrum allows one to deduce the plasma density at which the SRS is occurring (about 0.1–0.15 n_{cr} in this example).

The generation of high energy electrons is a very important nonlinear consequence of SRS. In this nonlinear optical process, part of the energy of the incident laser light is transferred into an electron plasma wave. In the nonlinear state, this plasma wave energy is damped into a tail of energetic electrons. The predicted correlation of hot electron generation with SRS has in fact been

confirmed in numerous experiments[5] in which Au disk targets were irradiated with 0.53 μm light with intensity $\geq 10^{15}$ W/cm^2. Figure 3 shows the fraction of the laser energy in hot electrons (as inferred from the concomitant hard x-rays) versus the measured fraction of the energy in Raman-scattered light. Note the excellent correlation which agrees with the expected partitioning of energy between the plasma wave and the scattered light wave.

The stimulated Raman reflectivity has been found to increase with plasma scale length, which is a key predicted trend. Figure 4 shows the measured peak Raman reflectivity versus the estimated density scale length.[3,6] In these experiments, the laser wavelength was ≤ 0.53 μm, and the nominal intensity was $>10^{15}$ W/cm^2. In the early experiments with disk targets, the scale length of the underdense plasma was rather small (~100 λ_0, where λ_0 is the laser wavelength) since the relevant intensity was achieved with a small focal spot. As lasers became more energetic, larger plasmas were created, both by using longer pulses and larger focal spots and by using thin foil targets which exploded and became transparent to the laser light. Using these latter targets, density scale lengths comparable to those expected in future inertial fusion reactor targets ($> 10^4 \lambda_0$) were achieved. Note that the peak Raman reflectivity indeed increased to a level $\geq 1/3$, which is near the maximum possible value if collisional absorption of the scattered light is taken into account.

Fortunately for inertial fusion, unsmoothed laser beams were used in these experiments. The Raman and Brillouin reflectivities of 0.35mm laser light from standard size gas-filled hohlraums have been found to be significantly reduced[7] with the addition of temporal and spatial incoherence. In these Nova hohlraum experiments, the ten laser beams were smoothed either with a kinoform phase

plate or with a phase plate plus smoothing by spectral dispersion using a bandwidth of 2.2 A. Figure 5 shows the reduction of the time-integrated reflectivities of a shaped pulse as the laser beam smoothing is increased. Work to improve the understanding of the scaling of SRS and SBS to larger ignition-scale plasmas and to uncover additional control mechanisms is ongoing. Direct drive targets remain an important option since the plasma then has a smaller scale length at ignition scale.

IV. RECENT EXAMPLES OF NONLINEAR INTERACTION PHYSICS

In the 1990's, experiments with both well-characterized plasma conditions and with well-defined laser beam statistics have become more common. Successful predictions are increasing. Recent examples include the suppression of filamentation by laser beam smoothing, laser beam spraying by filamentation, nonlinear laser beam bending in flowing plasmas, a dependence of the Raman reflectivity on ion wave damping, MeV electron generation by ultra-intense laser light, and significant energy transfer between crossing laser beams. Other examples could also be cited. Three of these examples will be discussed in more detail-examples chosen to represent experiments with small lasers, with large lasers, and with ultra-intense lasers.

A. Experiments with small lasers

Experiments with small lasers are extremely valuable for elucidating the underlying science. Since small lasers are relatively inexpensive to construct and operate, they can more readily explore parameter space with detailed

diagnostics and with good statistics. Recent experiments on nonlinear beam bending serve as an excellent example of contributions in this area.

Nonlinear beam bending was first predicted[8] as a consequence of filamentation in a plasma with flow transverse to the beam. The flow breaks the symmetry, and the most unstable filaments then occur at an angle. The effect maximizes when the transverse flow is sonic, since the plasma is then resonantly perturbed. This effect was proposed[9] to explain an enhanced laser beam deflection recently observed in experiments with hohlraums[10], a deflection investigated in more detail in Nova experiments with underdense foils.[11] Such a nonlinear beam bending can be very important for x-ray driven implosions, since the location of the laser energy deposition affects the symmetry of the x-ray drive on the capsule.

The basic physics of the nonlinear beam deflection was isolated and characterized in recent dedicated experiments[12] using the Janus facility. In these experiments the plasma was preformed by irradiating a thin disk with a 0.53 μm laser beam. The temperature, density and flow profiles of this plasma were then measured via interferometry and Thomson scattering. Finally a 1.06 μm interaction beam with a well-characterized intensity profile was propagated through the plasma at an angle to the plasma flow. These experiments were motivated by the predictions of a simple model[13] which treated the deflection as refraction in a nonlinearly-steepened density profile. The model emphasized that the enhanced deflection can even occur in the absence of filamentation (which of course would enhance the bending) and provided a prediction for the deflection angle as a function of plasma and laser parameters. In particular,

$$\theta \sim \frac{\ell_v}{4r_o}\frac{n}{n_{cr}}\left(\frac{v_{os}}{v_e}\right)^2 \qquad (3)$$

where ℓ_v is the velocity gradient length, r_0 the radius describing the intensity structure, n the plasma density where the transverse flow is sonic, n_{cr} the critical density, v_{os} the electron oscillatory velocity, and v_e the electron thermal velocity.

The beam deflection was directly observed via interferometric measurements of the density channel made by the beam. The beam was focussed with a cylindrical lens to facilitate these measurements. Interferograms are shown in Fig. 6 for two different intensities. The interaction beam, incident along the white arrow in each case, indeed deflects at a relatively low density where the measured transverse flow is near sonic. The channel formed by the deflected beam is apparent and denoted by the second arrow. For the upper higher intensity case, the observed deflection is about 10 degrees in agreement with the early predictions for this intensity. In addition, the deflection is clearly intensity-dependent as shown by the results in the second interferogram. It is very noteworthy that these experiments show deflection independent of filamentation, which is found to occur at another, significantly higher density in these experiments. Finally these well-diagnosed experiments have provided a detailed test bed for a three-dimensional wave propagation code (F3D).[14] Using the measured plasma and laser conditions, the calculations are in good agreement.

B. Experiments with large lasers

Sometimes large lasers are necessary in order to access plasma and irradiation conditions closer to future applications. For example, for inertial fusion, hohlraums for the National Ignition Facility will be filled with plasma with density near 0.1 n_{cr}, electron temperature > 4 keV, and density scale length > 3–5 mm. Since ignition targets are quite sensitive to nonlinear optical processes which affect symmetry, preheat, and shock timing, and since such processes have consistently been more difficult to control as the plasma size increases, it is clearly important to investigate the interactions in as large a plasma as possible. For this, experiments with large lasers are needed.

Recent investigations of the nonlinear behavior of SRS are an excellent example of interaction experiments with a large laser. In these experiments[15] large gas-filled hohlraums were irradiated with 0.35 mm light using the Nova laser. A large plasma was created with density near 0.1 n_{cr}, electron temperature about 3 keV, and plasma scale length about 2 mm. The ion wave damping of this plasma was varied by using different mixtures of gas. The Raman reflectivity of an interaction beam smoothed by a random phase plate and focused to an intensity > 2×10^{15} W/cm^2 was measured as a function of the ion wave damping. As shown in Fig. 7, the reflectivity varies with the ion wave damping, an effect independently found in Nova experiments[16] using gas-bag targets. This clearly demonstrates nonlinear saturation since the linear gain of SRS has no dependence on ion waves.

A nonlinear regime[17,18] in which the Raman reflectivity depends on ion wave damping had been predicted. In this case, the Raman-generated plasma wave becomes large enough to itself decay into another electron plasma wave

and an ion sound wave. This process is termed the Langmuir decay instability and can be represented as

$$\omega_{p1} \rightarrow \omega_{p2} + \omega_i \tag{4}$$

where ω_{p1} and ω_{p2} are frequencies of electron plasma waves and ω_i is the ion sound frequency. The simplest assumption is that this secondary decay very efficiently drains energy from the Raman-driven plasma wave, clamping its amplitude dn near the threshold of the secondary instability. The amplitude of the plasma wave at threshold would then be

$$\left(\frac{\delta n}{n}\right)^2 \sim 4k^2 \lambda_{DE}^2 \frac{\gamma_i}{\omega_i} \frac{\gamma_e}{\omega_p}, \tag{5}$$

where δn is the fluctuating density, n the plasma density, k the plasma wave number, λ_{de} the electron Debye length, and γ_i (γ_e) the ion wave (plasma wave) damping coefficient. Since the Raman relectivity is proportional to $(\delta n)^2$, this reflectivity would then vary with γ_i. Detailed calculations[18] using coupled rate equations indeed show such a dependence on the ion wave damping.

Finally our understanding of the nonlinear regimes continues to evolve. Simulations[19] of the saturation process have recently been carried out using a two-dimensional code solving the Zakharov equations to describe the plasma waves. These results indicate a need to invoke modified electron velocity distributions for the specific plasma conditions in the Nova experiments. Such a modification due to heating and electron heat transport have recently been proposed.[20] It should also be noted that there is another secondary instability which represents decay of a plasma wave into a light wave plus an ion sound wave.

C. Experiments with ultra-intense lasers

The last example addresses ultra-intense laser plasma interactions. With chirped pulse amplification[21], one can put a significant energy into short (< 1ps) laser pulses. These pulses have already been focussed to intensities up to 10^{21} W/cm^2. At such an intensity, the electron motion is highly relativistic. In particular,

$$\left(\frac{p_{os}}{m_o c}\right)^2 \simeq \frac{I\lambda_\mu^2}{1.4x10^{18}}, \tag{6}$$

where I is the intensity and λ_μ the laser wavelength in microns. Note that for 1.06 μm light with an intensity of 10^{21} W/cm^2, $p_{os}/mc \sim 30$. Likewise the light pressure is impressive: i.e.,

$$\frac{I}{c} \simeq 330\left(\frac{I}{10^{18}}\right) Mbar \tag{7}$$

At 10^{21} W/cm^2, the light pressure exceeds 300 gigabars.

Computer simulations using a particle-in-cell code were used to provide an early glimpse into this ultra-intense regime. As a simple example, consider a two-dimensional[22] simulation of a focussed light beam with intensity $I\lambda\mu m^2=10^{19}$ W-μm^2/cm^2 incident onto an overdense plasma. Over a third of the light was found to be absorbed into very energetic electrons. As shown by Fig. 8a, these electrons had an effective temperature of about 1 MeV, even at this intensity. As shown in Fig. 8b, the light pressure punched a hole in the plasma, causing it to recede at a significant fraction of the velocity of light. Both these effects have now been observed. It should be noted that the simulations also show self-generated magnetic fields with an amplitude up to 10^9 Gauss (for $I\lambda\mu m^2=10^{21}$ W-μm^2/cm^2).

Significant absorption of short, ultra-intense pulses into very energetic electrons has been demonstrated via measurements of K_α emission. In the experiments[23], a layered target was irradiated with 0.5ps pulses of 1.06 μm light focused to an intensity of about 10^{19} W/cm^2. Figure 9 shows the measured intensity of the K_α emission created by the electrons in a Molybdenum layer as a function of the thickness of a front layer of CH. When this data is fitted to code calculations including the electron transport and Ka excitation, an absorption of about 30% into electrons with an average energy between 330 and 600 keV is found.

D. Exciting challenges and promising developments

The interaction physics is clearly a very rich test bed for basic processes in ionized media. Much has been learned, and many exciting challenges remain. Quantitative calculations of nonlinear behavior remain the greatest challenge. These calculations are particularly difficult since important phenomena occur on very disparate space and time scales. For example, in inertial fusion applications, the time scales range from sub-femtosecond to nanoseconds, the space scales from sub-microns to centimeters. In addition, there's an intriguing interplay among different nonlinear processes. Fortunately, ongoing impressive advances in both plasma diagnostics and in computational capabilities bode well for the future.

Some recent experiments[24] in which gas bag targets were irradiated with 0.35 μm light using the Nova laser illustrate the rich nonlinear behavior. A range of plasma conditions was accessed. The electron temperature was about 3 keV, the plasma density varied from 0.06 to 0.15 n_{cr}, the ion wave damping from about

0.01 to 0.15 of the ion sound frequency. The laser intensity was about 2×10^{15} W/cm^2. As shown in Fig. 10, a striking anticorrelation between the stimulated Raman and Brillouin reflectivities was found. Such fascinating behavior is only partly understood.

Ongoing advances in diagnostics make laser plasmas an even better test bed for nonlinear processes. The increasing sophistication of the diagnostics is illustrated[25] in Fig. 11. In this example of a laser beam irradiating a preformed plasma, Thomson scattering is used to measure in space and time the amplitudes of both the ion sound wave due to SBS and the electron plasma wave due to SRS. Such remarkably detailed information both quantifies the complex coupled behavior of the plasma waves and allows detailed comparisons with theory and simulation.

Fortunately, rapid advances in computer models and computer power are also ongoing. A variety of three-dimensional codes that run on parallel machines have been recently developed. These include fully relativistic particle-in-cell codes[26], fluid electron, particle ion codes[27], as well as wave propagation codes[14,28], some including models for stimulated scattering. Codes for nonlocal heat transport and modified velocity distributions[29] and codes for the coupled Zakharov-quasilinear diffusion equations[19] are also now operative. Computer power continue to grow. In the last 20 years, the number of floating point operations per second has increased by a factor of about 10^4. A further increase of nearly two orders of magnitude is projected for the next 5 years, fueled by the Accelerated Scientific Computing Initiative. These advances will enable simulations on more realistic time and space scales.

V. Applications and summary

The interaction of intense lasers with matter spawns many applications. Very large ablation pressures can be created either by directly illuminating a target with laser light or by converting the light to x-rays which are used to heat and ablate the matter. In inertial fusion[30-32], these large ablation pressures are used to implode a capsule filled with DT. The implosion is hydrodynamically unstable, since one is in effect accelerating dense matter with a hot, tenuous plasma. The implosion must be rapid enough to avoid excessive growth of these hydrodynamic instabilities. This constraint places a lower limit on the ablation pressure and hence on the laser intensity. In turn, the interaction physics constrains the laser intensity from being too high in order to minimize stimulated scattering and other deleterious effects. Understanding how to optimally balance these constraints is the key to successful inertial fusion using lasers.

Impressive progress continues to be made in inertial fusion. The growth of hydrodynamic instabilities has been studied in numerous experiments, and excellent agreement with the modeling has been demonstrated.[33] In recent experiments with indirect drive using the Omega-upgrade laser at the University of Rochester, capsules with aspect ratios up to about 20 have been successfully imploded to give yields in good agreement with calculations.[34] With the National Ignition Facility, larger capsules with higher aspect ratios will be tested. NIF will provide a definitive test of inertial fusion.

Laser irradiation of matter allows many other applications. Various astrophysical phenomena can be investigated in the laboratory. For example, turbulent hydrodynamics can play a role in super-Novae explosions, an effect now being studied in scaled experiments[35] using lasers. Laser experiments also

allow investigation of many topics in high energy density physics. For example, the equation of state of Deuterium at high pressure has been measured. A significant modification of the equation of state due to molecular dissociation was found.[36]

Finally, there are applications which exploit the creation of intense plasma fields and energetic particles. The possibility of a laser plasma accelerator[37] is an exciting advanced application, which is leading to new understanding of many fundamental processes, such as optical guiding of laser pulses and electron acceleration in plasma waves. Other novel applications include the creation of high energy x-ray sources[38] and study of nuclear physics phenomena[39] using ultra-intense laser light.

VI. Acknowledgements

Work performed under the auspices of the U.S. Department of Energy by Lawrence Livermore National Laboratory under Contract W-7405-ENG-48.

This manuscript is based on an invited paper in a Centennial session at the American Physical Society meeting in March, 1999. I am grateful to numerous colleagues in the inertial fusion program. Special thanks to those who allowed me to show their data in this brief overview of laser matter interactions at the end of the 20th Century.

References:

1 Laser Programs: The First 25 Years....1972–1997. Lawrence Livermore National Laboratory UCRLTB–126043, available from National Technical Information Service 5855 Port Royal Road, Springfield, VA 22161

2 K. Mima and K. Nishikawa, in Handbook of Plasma Physics, Vol. 2 (North Holland, Amsterdam,1984), p. 452-517, and many references therein

3 H.A. Baldis, E.M. Campbell, and W.L. Kruer; in Handbook of Plasma Physics, Vol. 3 (North Holland, Amsterdam, 1991), p 361-434, and many references therein

4 W. Seka, E.A. Williams, R.S. Craxton, L.M. Goldman, R.W. Short, and K. Tanaka, Phys. Fluids **27**, 2181 (1984)

5 R.P. Drake et al., Phys. Rev. Letters 53,1739(1984), S.J. Kartunnen, Phys. Rev. A23,2006(1981)

6 C.B. Darrow, R.P. Drake, D.S. Montgomery, P.E. Young, K. Estabrook, W.L. Kruer, and T.W. Johnston, Phys. Fluids B2,1473(1991)

7 S.H. Glenzer et al., Phys. Rev. Letters 80,2845(1998)

8 R.W. Short, R. Bingham, and E.A. Williams, Phys. Fluids 77,2302(1982)

9 H.A. Rose, Phys. Plasmas 3,1700(1996); D.E. Hinkel, E.A. Williams, and C.H. Still, Phys. Rev. Letters 77,1298(1996)

10 R.L.Kauffman et. al., Phys. Plasmas 5,1927(1998)

11 J.D. Moody, B.J. MacGowan, D.E. Hinkel, W.L. Kruer, E.A. Williams, K. Estabrook, R.L. Berger, R.K. Kirkwood, D.S. Montgomery, and T.D. Shepard, Phys. Rev. Letters 77,1294(1996)

12 P.E. Young, C.H. Still, D.E. Hinkel, W.L. Kruer, E.A. Williams, R.L. Berger, and K.G. Estabrook, Phys. Rev. Letters 81,1425(1998)

13 W.L. Kruer and J. Hammer, Comments Plasma Phys. Cont. Fusion 18,85(1997)

14 R.L. Berger, B.F. Lasinski, T.B. Kaiser, E.A. Williams, A.B. Langdon, and B.I. Cohen, Phys. Fluids B5,2243(1993)

15 J.C. Fernandez et al., Phys. Rev. Letters 77,2702(1996)

16 R.K. Kirkwood et al., Phys. Rev. Letters 77,2706(1996)

17 . R.P Drake and W. Batha, Phys. Fluids B3,2936(1991)

18 B. Bezzerides, D.F. DuBois, and H.A. Rose, Phys. Rev. Letters 70,2569(1993), J.T. Kolber, W. Rozmus, and V.T. Tikhonchuk, Phys. Fluids B5,138(1993)

19 D. Russell, et al., private communication (1998)

20 B.B. Afeyan A.E. Chou, J.P. Matte, R.J. Towm, and W. L. Kruer; Phys. Rev. Letters 80,2322(1998)

21 M.D. Perry and G. Mourou, Science 264,917(1994)

22 S.C. Wilks, W.L. Kruer, M. Tabak, and A. B. Langdon, Phys. Rev.Letters 69,1383(1992)

23 K.B. Wharton, S.P. Hatchett, S.C. Wilks, M.H. Key, J.D. Moody, V. Yanovsky, A.A. Offenberger, B.A. Hammel, M.D. Perry, and C. Joshi, Phys. Rev. Letters 81,822(1998)

24 D.S. Montgomery, et al., Phys. Plasmas 5,1973(1998)

25 C. Labaune, H.A. Baldis, et al., Phys. Plasmas 5,234(1998)

26 A. Pukhov and J. Meyer-ter-Vehn, Phys. Rev. Letters 77,3975(1996)

27 H.X. Vu, J. Comput. Phys.124,417(1996)

28 A. J. Schmitt, Phys. Fluids b3, 186(1991)

29 J.P. Matte, Plasma Phys. Control. Fusion 30,1665 (1988)

30 .H. Nuckolls, L. Wood, aq. R. Thiessen, and G.B. Thiessen, Nature 239,139 (1972)

31 S.E. Bodner, J. Fusion Energy 1,121 (1981)

32 J.D. Lindl. Phys. Plasmas 2,3933 (1995)

33 S.G. Glendinning et. al., Phys. Rev. Letters 78,3318 (1997)

34 P.Amendt, Bull. Am. Phys. Soc. 43,1739 (1998)

35 B. Remington et al., Phys. Plasmas 4,1994 (1997)

36 L.B. Da Silva et. al., Phys. Rev. Letters 78,483 (1997)

37 C. Joshi, et al., Nature 311,525 (1984)

38 W.L. Kruer, E.M. Campbell, C.D. Decker, S.C. Wilks, J. Moody, T. Orzechowski, L. Powers, L.J. Suter, B.B. Afeyan, and N. Dague, Plasma Phys. Control. Fusion 41, 1777 (1999)

39 T. Cowan, et al., submitted to Phys. Rev. Letters (1999)

Figure captions:

Figure 1. A collage showing high power glass lasers developed in the inertial fusion program at the Lawrence Livermore National Laboratory.[1]

Figure 2. A representative measurement of the intensity of Raman scattered light versus wavelength.[4]

Figure 3. The fraction of the laser energy into high energy electrons as inferred from hard x-rays versus the fraction of the energy into Raman-scattered light.[5]

Figure 4. The largest measured time-integrated Raman reflectivity versus density scale length in units of the laser wavelength. The targets were either disks or foils irradiated with either .53mm or .35mm light as indicated.[3,6]

Figure 5. Dependence on laser beam smoothing of the time-integrated Raman and Brillouin refectivities measured in CH-filled, Nova hohlraums irradiated with a shaped pulse on the laser beam smoothing.[7] The laser beams were focused with f/4 optics and were unsmoothed (no KPP), smoothed with a phase plate (KPP), or smoothed with both a phase plate and SSD, as indicated.

Figure 6. Interferograms that show the channel formed by the interaction beam for peak intensities of either 1.5×10^{15} W/cm^2 (upper) or 1×10^{15} W/cm^2 (lower).[12]

Figure 7. The time-integrated reflectivity measured from large toroidal gas-filled hohlraums versus the ion wave damping.[15] In these experiments, the Nova laser beams were focused with an f/4 lens,and the interaction beam was smoothed with a random phase plate.

Figure 8. A spectrum of the energy distributions of the heated electrons (left) and a snapshot of the positions of the plasma electrons, showing the surface deformation (left).[22]

Figure 9. Intensity of the measured Ka emission as a function of the thickness of the front layer in g/cm2.23.

Figure 10. The peak Brillouin reflectivity versus the Raman reflectivity at this time as measured in numerous experiments in which gas bag targets are irradiated with the Nova laser.[24]

Figure 11. A schematic showing measurements in space and time of the ion sound waves and electron plasma waves in a laser-irradiated preformed plasma.[25]

Figure 12. A photograph showing the National Ingnition Facility as of January 17, 1999.

Janus (1974)

Argus (1976)

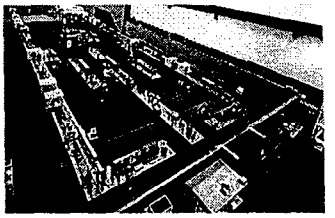

Shiva (1977)

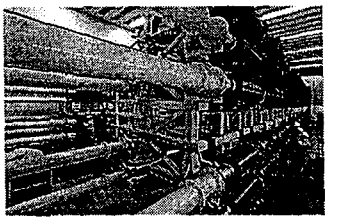

Novette (1983)

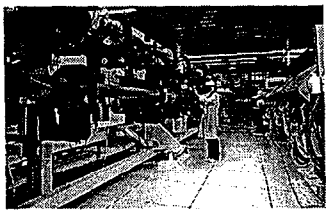

Nova (1984)

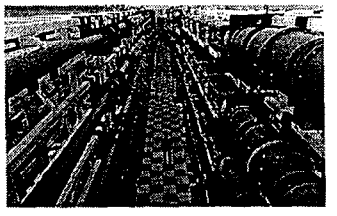

Beamlet—NIF prototype beamline (1994)

National Ignition Facility

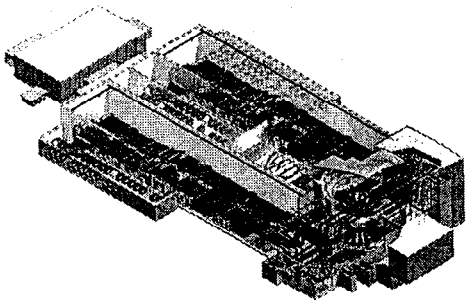

40-00-0295-0469Tpb01
13WJH/dsm/geg

4/21/99
RRJ/mcm

Fig. 1

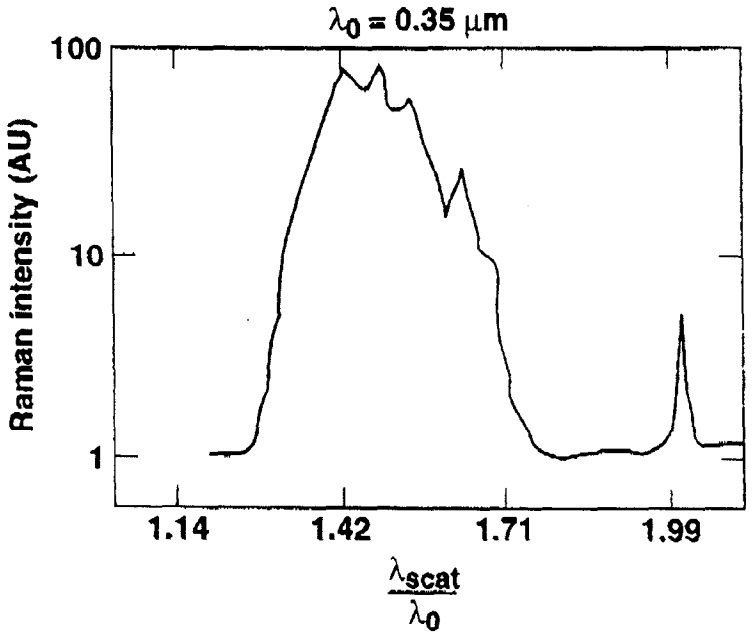

50-00-0190-1122A
22WLK/mcm

4/21/99
RRJ/mcm

FIG 2

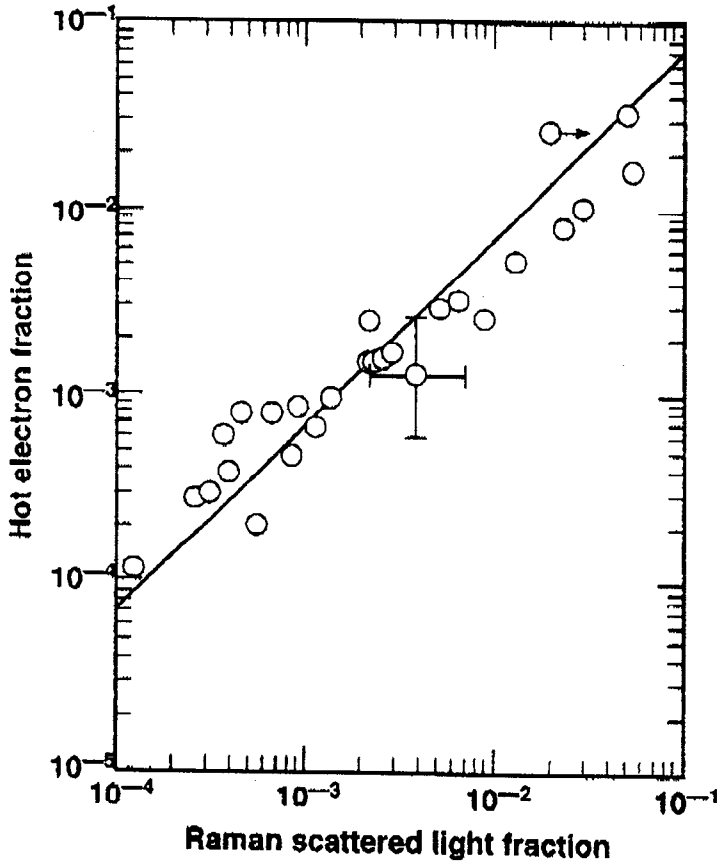

30-00-0791-2917AD001
22WLK

4/21/99
RBJ/mcm

Fig 3

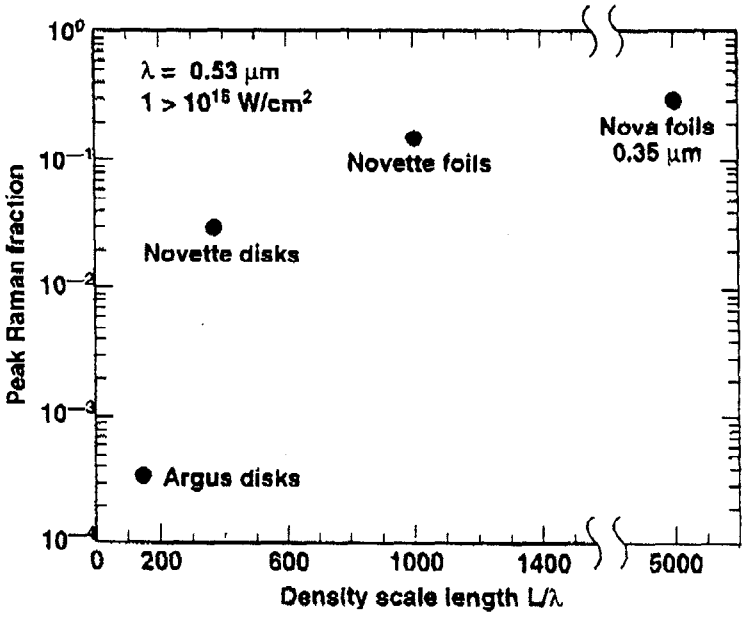

50-00-0791-2917Apb02
22WLK

4/21/99
RRJ/mcm

F16 4

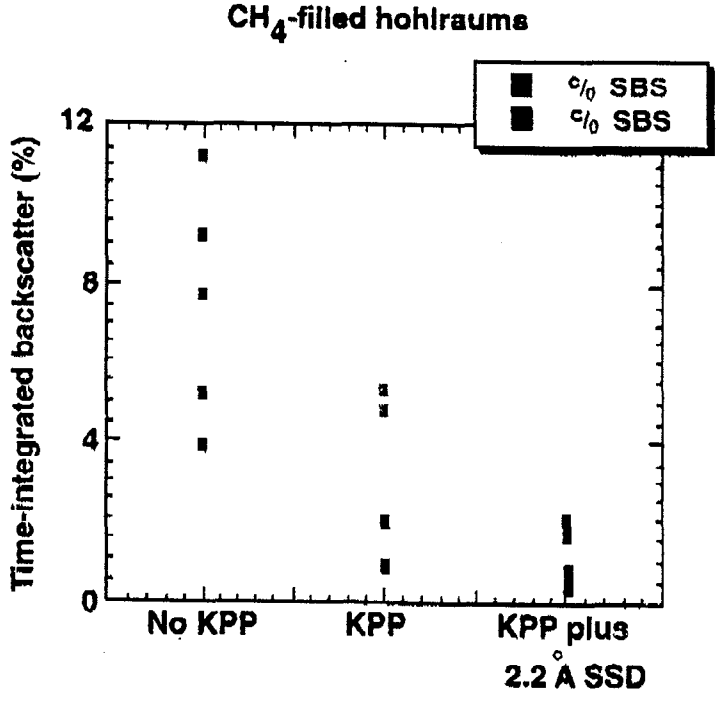
CH4-filled hohlraums
c/0 SBS
c/0 SBS
Time-integrated backscatter (%)
12
8
4
0
No KPP
KPP
KPP plus
2.2 Å SSD
50-00-0399-0413pb01
BWLK/kjm
4/21/99
RRJ/mcm

Fig 5

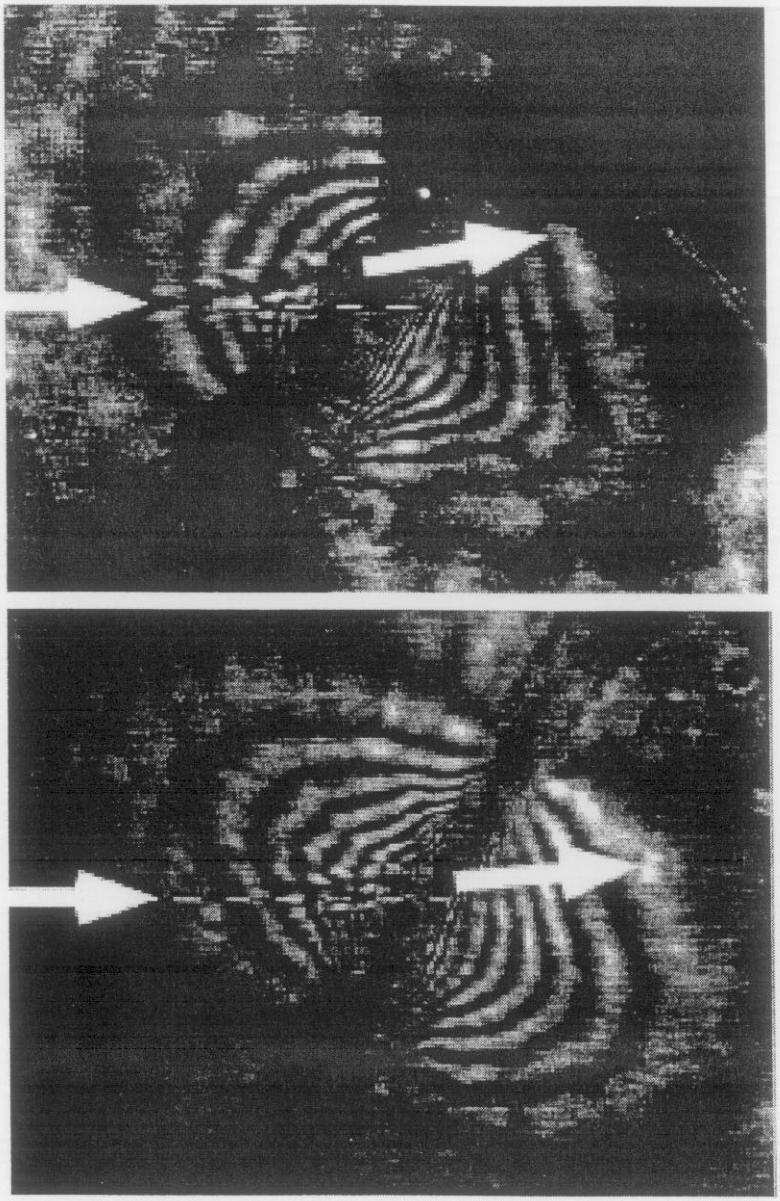

50-00-0399-0562pb01
8WLK/kjm

4/21/99
RRJ/mcm

Fig. 6

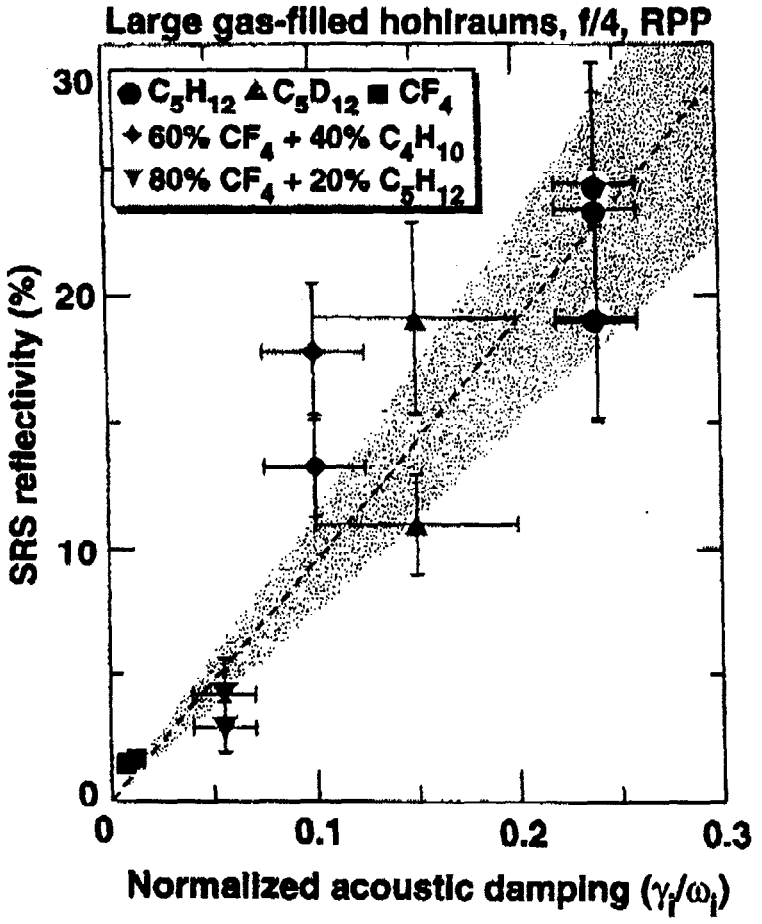

50-00-0399-0524pb01
1WLK/erm

4/21/99
RRJ/mam

Fig 7

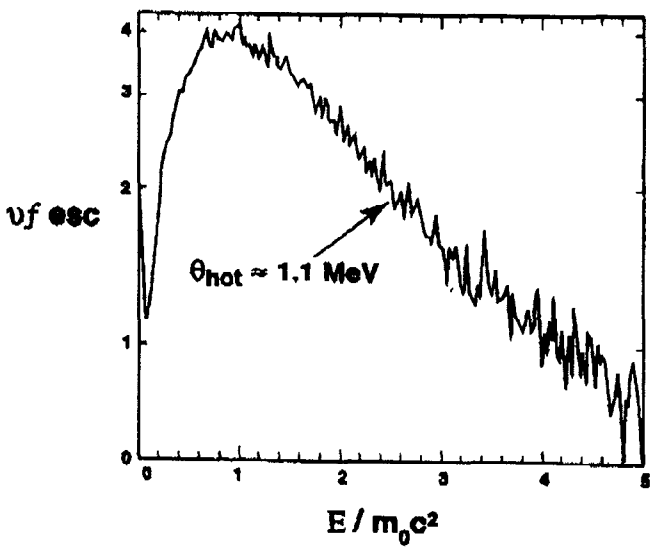

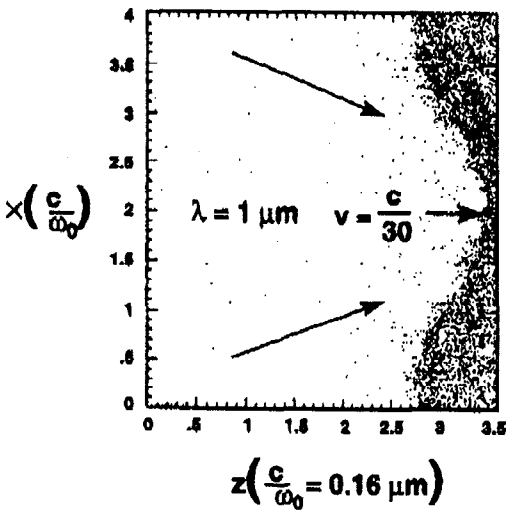

50-00-0399-0412pb01
SWLK/kjm

4/21/99
RRJ/mcm

Fig 8

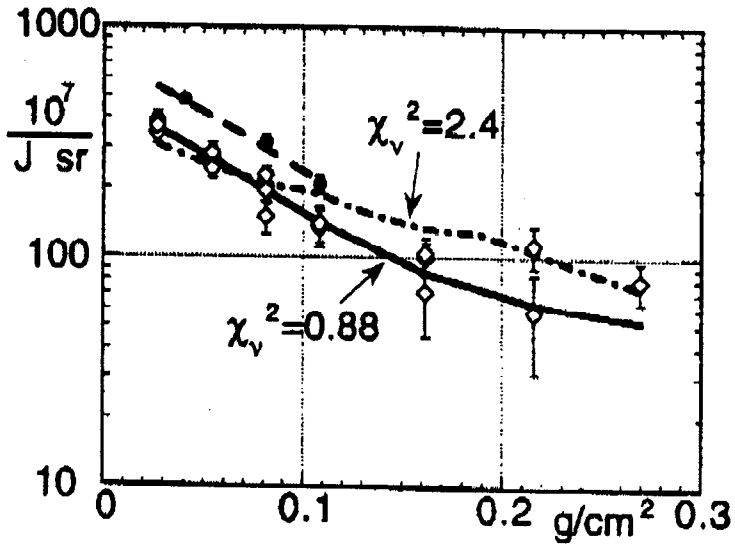

50-00-0399-0561pb01
SWLK/djm

4/21/99
RRJ/mcm

Fig 9

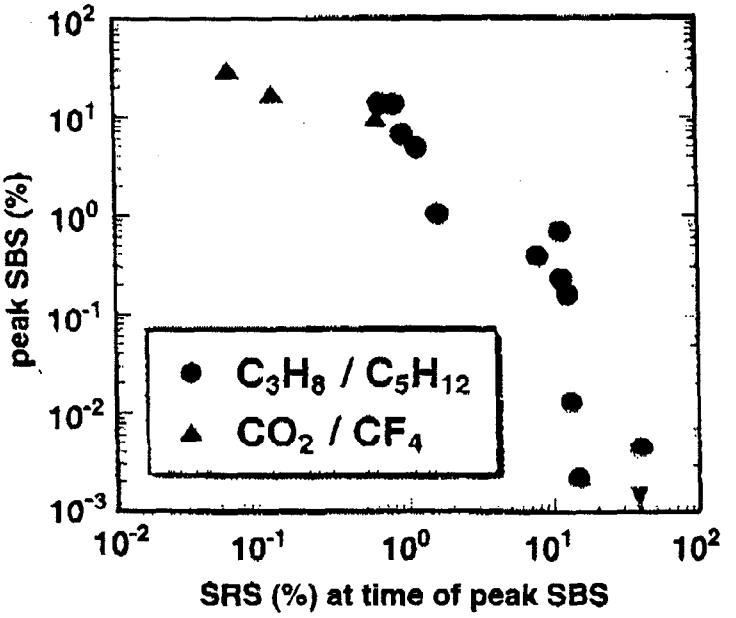

50-00-0399-0594pb01
15WLK/kjm

4/21/99
RRJ/mcm

FIG 10

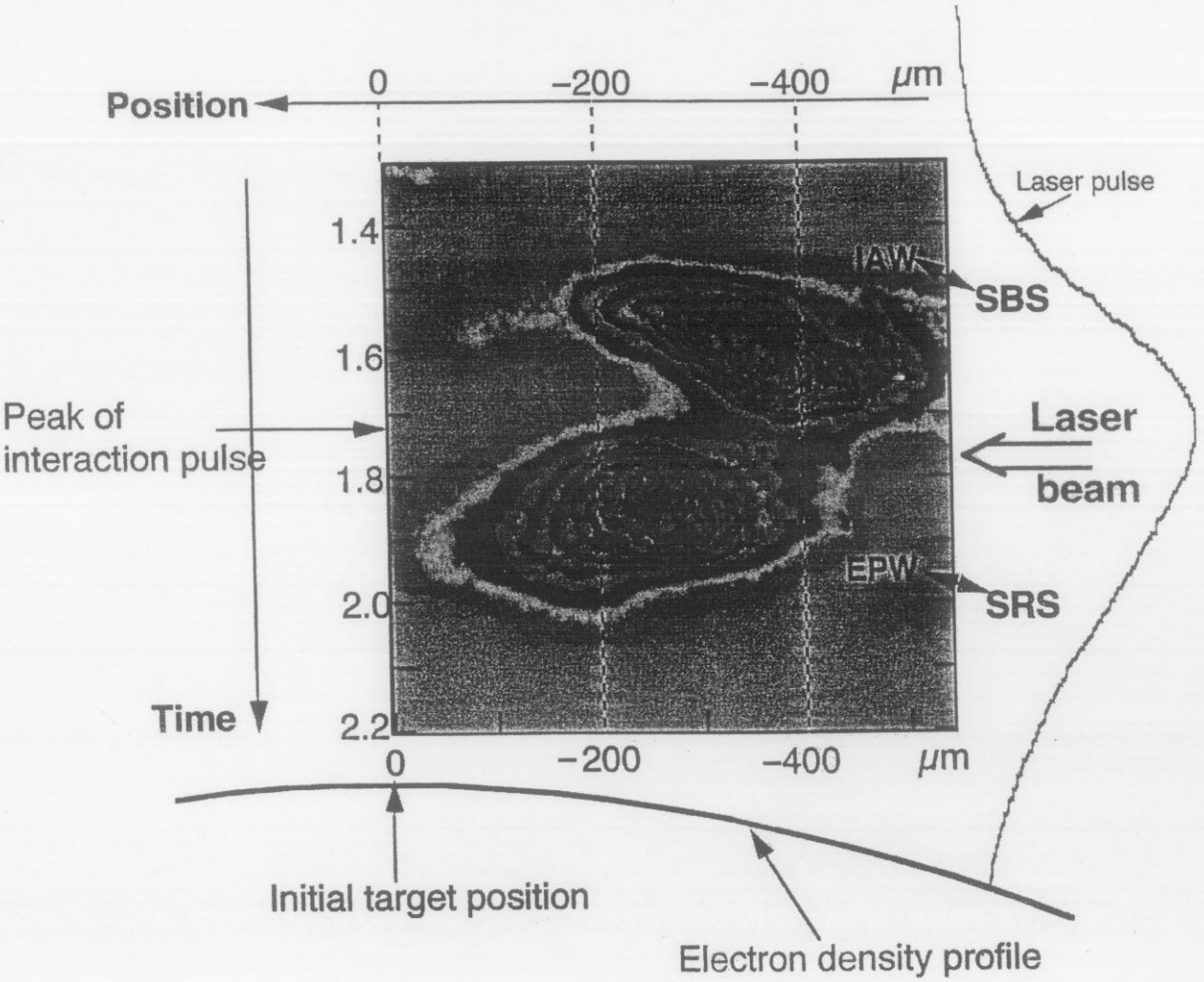

50-00-0399-0564pb01
8WLK/kjm

4/21/99
RRJ/mcm

Fig. 11

40-60-0199-0167#3pb01
27JAP/cld

4/21/99
RRJ/mcm

Fig. 12